Journal of Kerbala University , Vol. 8 No.1 Scientific . 2010

Finite Element Analysis of Non-Prismatic Prestressed Concrete Double Tee Beams

تحليل العتبات الخرسانية مسبقة الإجهاد غير الموشورية ثنائية الجذع باستخدام طريقة العناصر المحددة

د. احسان الشعرباف
كلية الهندسة-جامعة النهرين

د. خالد محمود شاكر
كلية الهندسة-جامعة بغداد

د. حسام علي محمد
الكلية التقنية-المسيب

Abstract

This research deals with the nonlinear finite element analysis of non-prismatic prestressed concrete double tee beams under flexure. The numerical analyses have been carried out on beams chosen from the available experimental studies.

Two different setups were considered. Beams B2 and B3 were experimentally tested by Mohammed 2003 and meant to represent the case of a non-prismatic prestressed concrete double tee beam. Beam B3, in particular, represents a beam with a short span. Beam B2, on the other hand is a sample for a relatively long span beam. These two beams were tested up to failure.

The finite element results are compared with the results of the available experimental tests. Parametric studies have been carried out throughout this study to investigate the effect of some important material and solution parameters on the numerical results. Effects of concrete compressive strength, amount of prestressing steel reinforcement, and initial prestressing forces are studied. A mathematical model suitable for the nonlinear analysis of prestressed concrete beams under monotonically increasing load is used. The validity, accuracy, and efficiency of the computational model are examined by comparing the finite element results with the experimental results.

الخلاصـــة

تناول البحث المقدم تحليل مجموعة عتبات خرسانية مسبقة الصب و الإجهاد متغيرة المقطع طولياً ثنائية الجذع تحت تأثير أحمال الانحناء حيث تم اختيار مجموعه من هذه العتبات من الفحوص المختبرية العملية و بإبعاد حقيقية لتكون موضع الدراسة.

تكرست الدراسة على عتبتان مسبقتا الصب و الاجهاد اختيرت من الفحوص العملية و المتضمنة: B2 و B3 و المفحوصة في شركة الرشيد العامة للمقاولات المحدودة عام 2003. اعتمدت العتبة الخرسانية B3 لتمثل العتبات القصيرة نسبياً بينما اعتمدت العتبة B2 لتمثل العتبات الطويلة, حيث تم فحص كل من هاتين العتبتين حتى الفشل. تم تحليل كل من هذه العتبات باستخدام طريقة العناصر المحددة و قورنت النتائج مع قريناتها في الجانب العملي. بشكل عام لوحظ التوافق بين النتائج المستحصلة لكل من هذه العتبات خلال مراحل الانتقالية للتحميل. كذلك تم دراسة العديد من المتغيرات الخاصة بالمادة وطريقة العناصر المحددة لمعرفة تأثيرها. كما درس تأثير مقاومة الانضغاط الخرسانية وكمية التسليح و... الخ.

Introduction

Double tees offer beauty and flexibility in design. These precast/prestressed concrete units are ideal for floor and roof systems requiring long, uninterrupted spans and extra heavy load carrying capabilities [1]. The remarkable strength of a double tee is the result of a design and manufacturing system that uses the best attributes of steel and concrete. Double tees are recommended for consideration for longer spans and heavier loads which exceed the capacity of hollow core slabs.

In the literature, many researchers consider the double tee section, experimentally and analytically as **In 1974 Wright and Burns** [2]studied the general load-deflection characteristics through ultimate of standard double tee and hollow-cored slab sections. A numerical analysis has

been carried out for members designed following ACI 318-71. **In 1989,Burnley and Aswad** [3]conducted two static load tests on full scale,3.05m wide, double tees. The specimens were typical production double tees spanning 18.9 m. **In 1990,El Shahaw**y,[4]studied the feasibility of using a prestressed double tee concrete system in bridge structures with spans up to 24.4m. **In 1992 the Consultant Office of Al-Basra University** [5] tested experimentally 16m span non-prismatic ordinary reinforced concrete beam according to the request of Al-Fayhaa Company for Precast Unit. The test specimen is a 2390mm wide beam,with a 500mm depth at supports and 800m at mid-span. **In 1999,Tadros *et al*.,**[6]published a report that presents a method for designing prestressed precast reinforced concrete double-tee joists with web openings. **In 1999,Nass,**[7]worked on computer programming to design a user-friendly worksheet capable of designing double-tee sections using Mathcad 7.0 Professional Edition. **The National Center for the Construction Laboratories** [8] tested experimentally a piece of ordinary reinforced concrete double tee beam on **2002** following the request of Karbala Company for Precast Concrete Unit. From final outlook, the beam has been tested experimentally for a full loading-unloading cycle under flexure. **In 2003,Grace *et al*.,**[9]presented a study on the fabrication, instrumentation, and flexural testing of a full-scale double-tee beam, prestressed using bonded pretensioned CFRP Leadline tendons and unbounded carbon fiber composite cable (CFCC) post-tensioning strands. **In 2004,Nanni and Casadei,**[10]presented a study examine experimentally three double tee beams up to failure, where two double tee prestressed concrete beams were strengthened with SRP composite materials and a third beam was tested as control specimen.

Up to the author's knowledge and survey, no experimental research has been found on prestressed non-prismatic double tee beams. On that base the major priority of this research will be pointed on the prestressed non-prismatic double tee beams.

Outline of the Adopted Computer Program

In the present study, the computer program 3DNFEA (3-DimensionalNon-linear Finite Element Analysis)which was originally developed by Al-Shaarbaf [11] has been used. This program was constructed mainly for the non-linear analysis of reinforced concrete members under general three-dimensional state of loading up to failure. In this study, the computer program 3DNFEA has been adopted for analyzing prestressed concrete beams. It was been modified to be suitable for analyzing prestressed concrete beams. The steps required by the computer program analyze prestressed concrete double tee non-prismatic beams are:

1.Read the structural data, material properties and tendon geometry. **2.**Read the number of sampling points that represent the prestressing tendons in addition to the value of effective prestressing stress and strain **(**f_{se},ε_{se}**)**respectively. **3.**Read the number of all sampling points, which represents the prestressing tendons. **4.**Then the effective prestress and prestrain are introduced to the prestressing sampling point by means of successive increments of loading. **5.**Check whether convergence has been achieved for that particular load increment. **6.**When the prestressing stress has been fully introduced, the external vertical loads are then applied at non-uniform increments. Large increments were used at the first stages of loading, while appreciably small-increments were used for stages close to the ultimate load.

Constitutive Relationships and Finite Element Formulation

Reinforced and prestressed concrete, are usually simulated by considering the constitutive relations of its constituents independently, because each of concrete and prestressing and reinforcing steel have very different material properties. The *20-noded isoparametric brick element* was used to model the concrete and both prestressing and reinforcing bars was idealized and axial members embedded within the concrete elements, as shown in **Fig. (1)**.

The behavior of concrete in compression was simulated by an ***elastic-plastic work hardening model*** followed by a perfectly plastic response, which is terminated at the onset of crushing as shown in **Fig. (2)** [11]. In tension, a ***smeared crack*** model with fixed orthogonal cracks was used with the inclusion of models for the retained post-cracking stress and reduced shear modulus as shown in **Fig. (3, and 4)**.

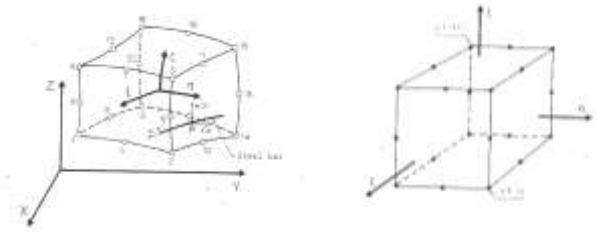

Fig. (1). The 20-noded isoparametric brick element [11].

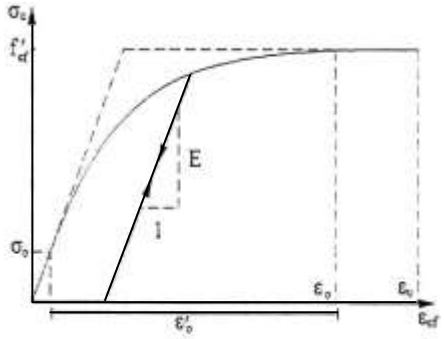

Fig. (2). Uniaxial stress-strain curve for concrete.

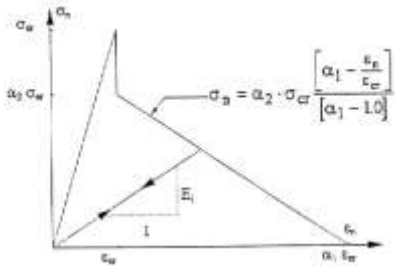

Fig.(3). Tension-stiffening model for concrete [11].

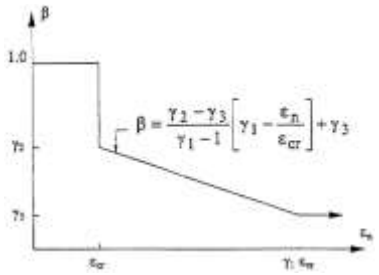

Fig.(4). Shear Retention model for concrete [11].

Slenderness of steel allows generally assumed to be capable of transmitting axial force only. An elastic linear work hardening model is used to represent the uniaxial stress-strain behavior of the reinforcement, as shown in **Fig. (5)** [11].

The nonlinear equations of equilibrium were solved using an incremental-iterative technique operating under load control. The ***standard and modified Newton-Raphson*** methods were used as solution algorithms [11].

Full details of the constitutive models and the finite element formulation can be founded in reference [12]

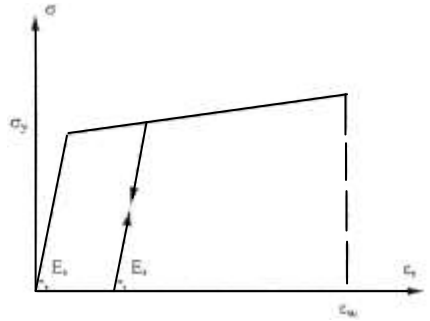

Fig. (5). Stress-strain relationship of steel bars used in the analysis.

Tested Prestressed Double Tee Beam B2

The beam B2 was numerically analyzed using the finite element model presented in this work. This beam was experimentally testes up to failure and also analyzed, where full details founded in reference [12]. General dimensioning and isometric view shown in **Fig. (6)**, and **Fig. (7)**.

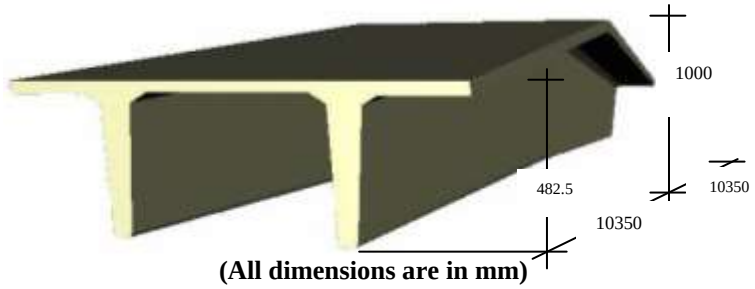

(All dimensions are in mm)

Fig. (6). Beam B2 – Isometric view and dimensioning.

Finite Element Idealization and Material Properties

By taking into consideration the advantage of geometric and loading symmetry, a segment which represents one quarter of the beam has been used in the finite element analysis. The chosen segment was modeled using the 20-node isoparametric hexahedral brick elements. This quarter was discretized into 10 brick elements. The uniformly distributed load was modeled using equivalent nodal loads distributed at top face of the flange. The finite element mesh, boundary and symmetry conditions, and loading arrangement are shown in **Fig. (8)**. Material properties used in the analysis are listed in **Table (1)**.

The finite element analyses have been generally carried using the 27-point rule, with a convergence tolerance of 4%. The modified Newton-Raphson method in which the stiffness matrix is updated at the second iteration of each increment of loading has been adopted as a nonlinear solution algorithm. Non-uniform increments have been used for applying the external loads. Large increments were used at the first five stages of loading, and then appreciably smaller increments were used for stages close to ultimate load.

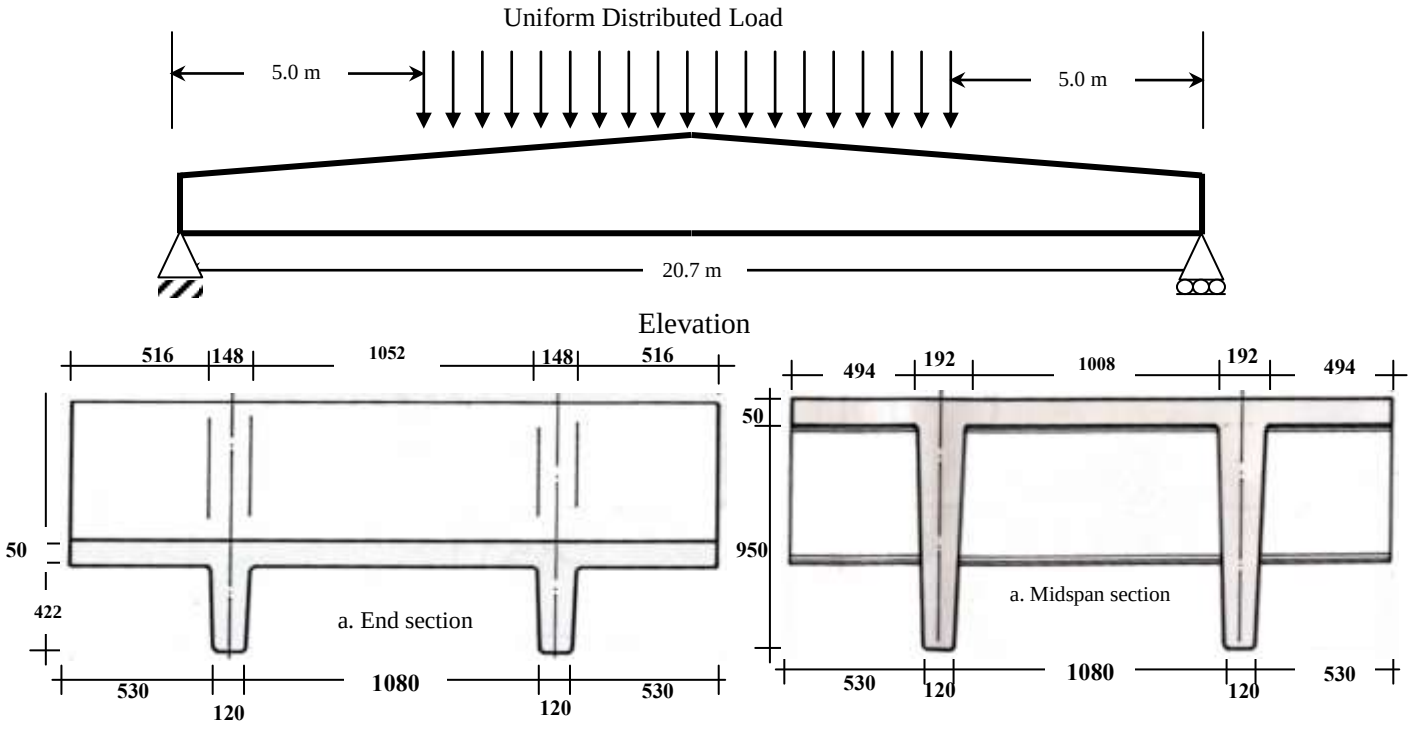

Fig. (7). beam B2 - dimensions and loading arrangement.

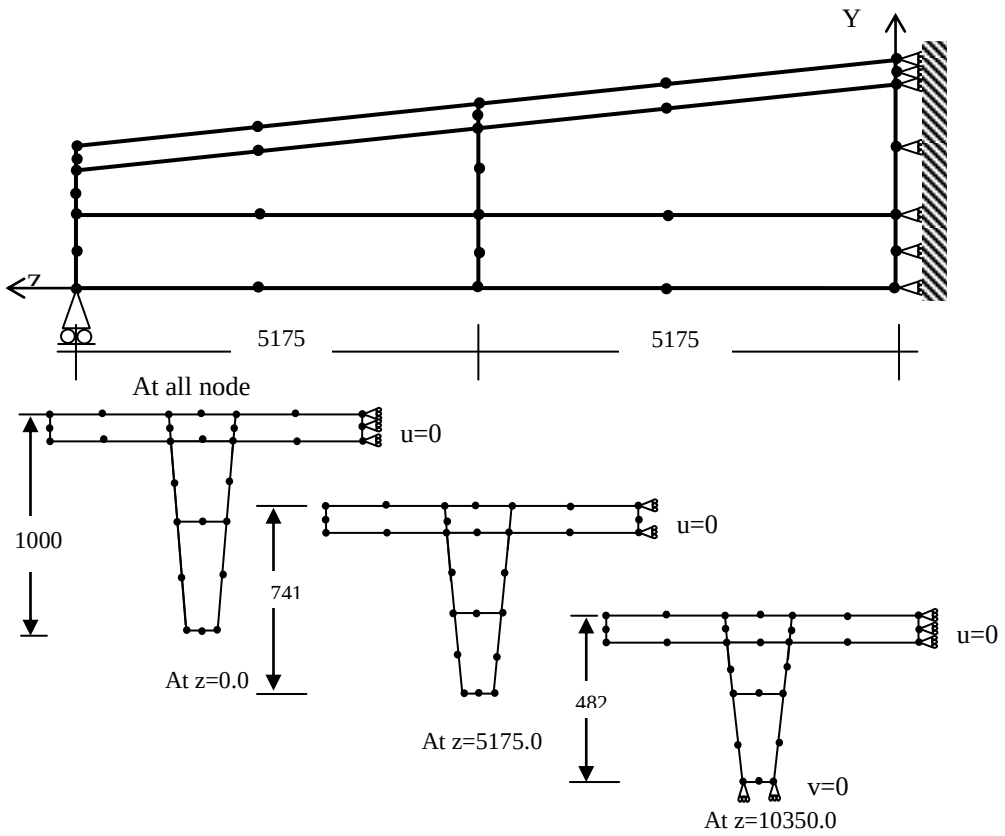

Fig. (8). Beam B2- finite element mesh, boundary and symmetry conditions used in the analysis.

Table (1). Beam B2 - Material properties used in the analysis.

Concrete		**Prestressing tendons**	
Young's modulus E (N/mm2)*.	**31200**	**Young's modulus Es (N/mm2)†.**	**200000**
Compressive strength fc' (N/mm2)	**45**	**Effective prestressing stress (N/mm2).**	**1117**
Tensile strength ft (N/mm2)**	**4.15**	**Yield stress (N/mm2).**	**1650**
Poisson's ratio, υ†	**0.2**	**Area of prestressing tendon (mm2)**	**1718**
Non-prestressing bars			
Young's modulus E_s (N/mm^2) †	**200000**		
Yield stress f_y (N/mm^2)	**450**		
Area of steel, (mm^2)	**628**		

* $E_c=4700\sqrt{f'_c}$ ** $f_t=0.62\sqrt{f'_c}$ †Assumed value

Beam B2- Results of Analysis

Figure (9) shows the experimental and numerical load deflection curves obtained for this beam. The figure indicates good agreement for the finite element solutions compared with the experimental results throughout the entire range of behavior. The figure reveals that the obtained final deflection is slightly greater than the corresponding experimental deflection. The computed load-deflection curve is almost similar to the experimental results. **Table (2)** shows predicted cracking and ultimate loads obtained using the different methods. The ultimate load obtained by the finite element method is higher than the experimental value by 2.47%.

Table (2) Beam B2 - Predicted cracking and ultimate loads.

Prestressing pattern	*Cracking load (kN)*	*Ultimate load (kN)*
Experimental	*68*	*222*
F.E.M	*72*	*227.5*

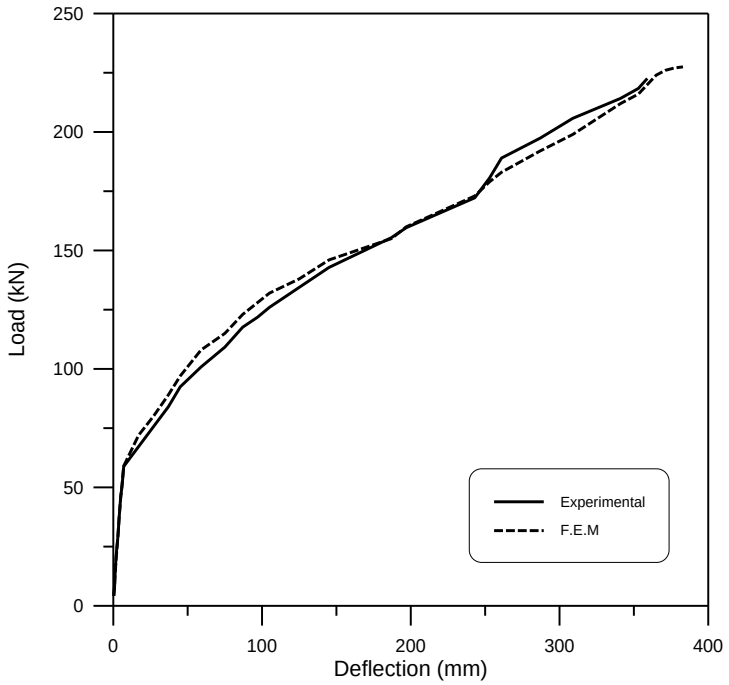

Fig. (9). Beam B2- numerical and experimental total load-midspan deflection behavior.

Tested Prestressed Double Tee Beam B3

Also, beam B3 has been experimentally tested up to failure and chosen as a second case [13]. This beam was numerically analyzed using the nonlinear finite element model presented in this research work. General outlook of the beam is shown in **Fig. (10)**. The elevation and specified selected cross-sections and dimensioning are illustrated in **Fig. (11)**.

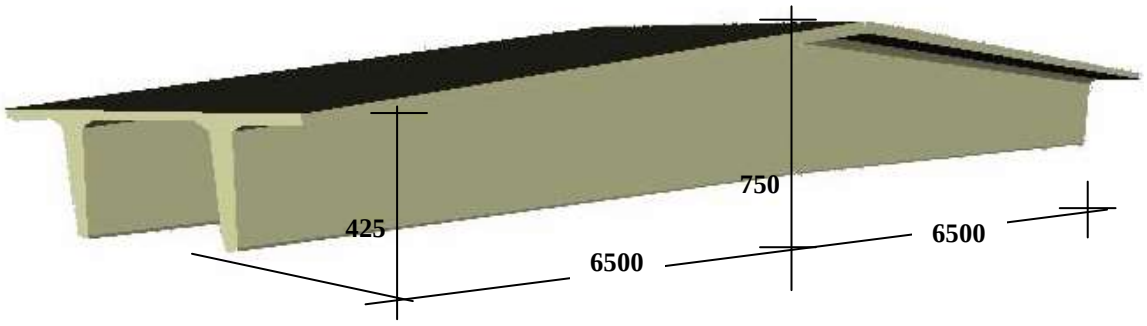

(All dimensions are in mm).

Fig. (10). beam B3 – Isometric view and dimensioning.

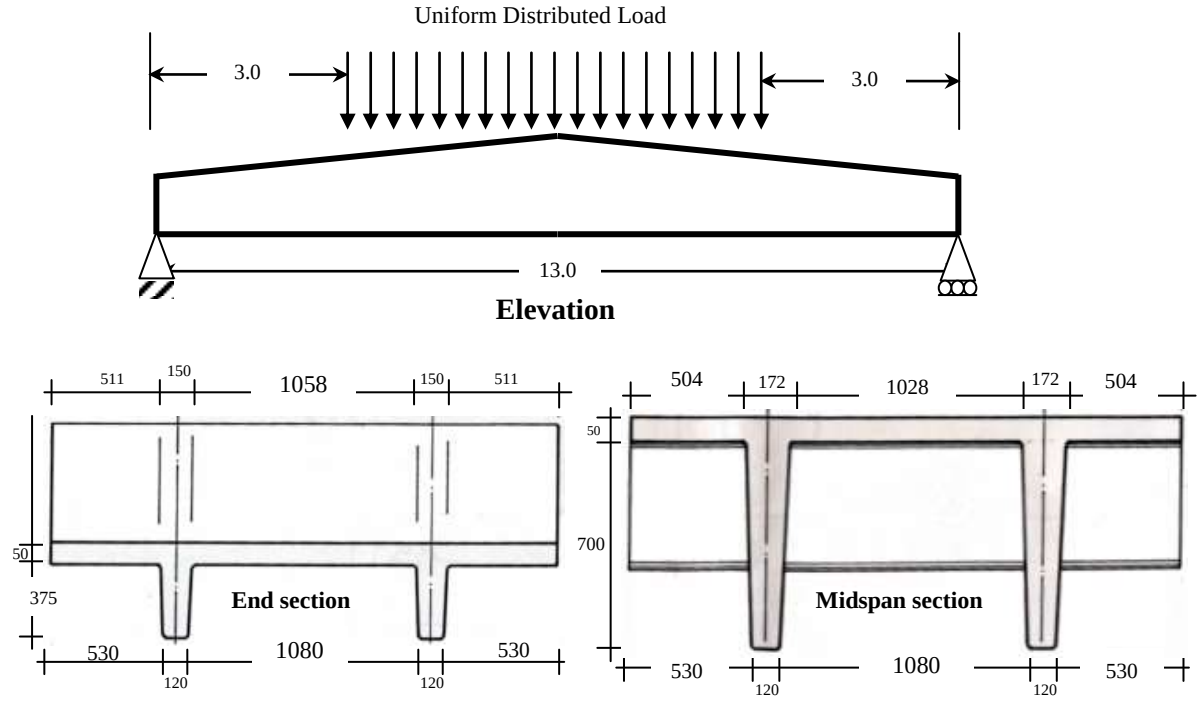

Fig. (11). Beam B3 - Dimensions and loading arrangement.

Finite Element Idealization and Material Properties

As was the case with the finite element model in the foregoing analyses, loading and geometric symmetry were utilized for an advantage by reducing the problem to analyze only one quarter of the beam. Again, 10-node isoparametric hexahedral brick elements were used. The uniformly distributed load on the beam surface were represented by a statically equivalent set of nodal forces, all subjected on the flange. The finite element mesh, boundary and symmetry conditions and loading arrangement are shown in **Fig. (12)**.

The finite element analyses have been carried out using the 27-point rule, with a convergence tolerance of 5%. The modified Newton-Raphson method in which the stiffness matrix is updated at the second iteration of each increment of loading has been adopted as a nonlinear solution algorithm. Before applying the external load, an effective prestressing stress and strain are introduced to the sampling points representing the prestressing tendons by means of successive increments. Then non-uniform increments have been used for applying the external load. Large increments were used at the first five stages of loading, and then appreciably smaller increments were used for stages close to the ultimate load.

The material properties used in the finite element analysis are shown in **Table (3)**. Beam B3 contained 3 wire strands in each rib, providing 576mm^2 prestressing area, yielded on 1650 N/mm^2. These strands having an effective prestressing stress of 1117N/mm^2,

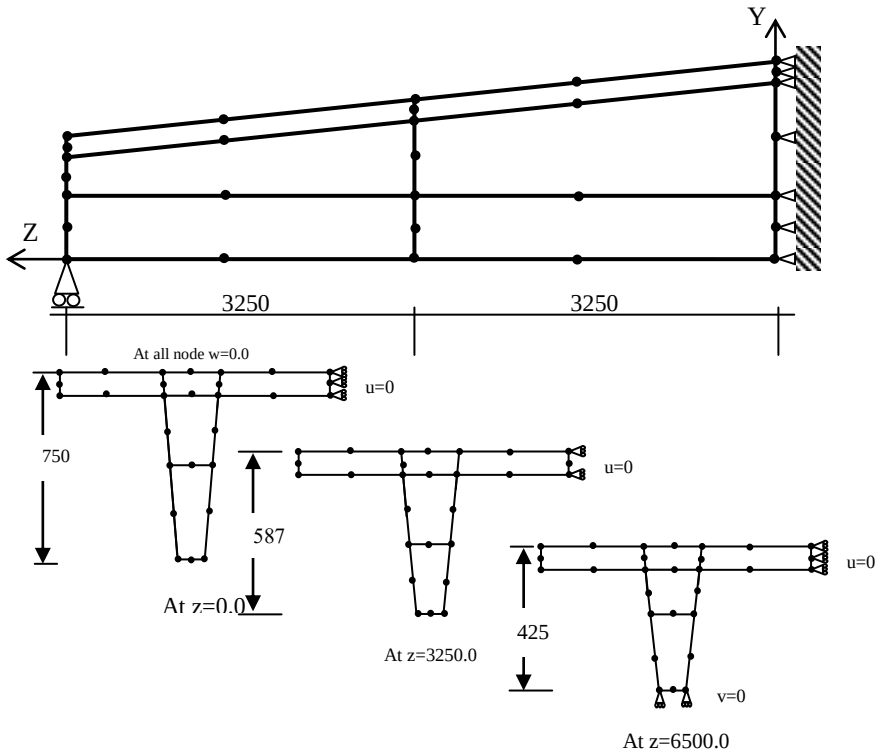

Fig. (12). Beam B3- finite element mesh, boundary and symmetry conditions used in the analysis.

Table (3). Beam B3 - Material properties used in the analysis.

Concrete		**Prestressing tendons**	
Young's modulus E (N/mm^2)*.	30094	Young's modulus E_s (N/mm2) †.	200000
Compressive strength fc' (N/mm^2)	41	Effective prestressing stress (N/mm2).	1117
Tensile strength f_t (N/mm^2)**	3.96	Yield stress (N/mm2).	1650
Poisson's ratio, ν†	0.2	Area of prestressing tendon (mm2)	756
Non-prestressing bars			
Young's modulus E_s (N/mm^2) †	200000		
Yield stress f_y (N/mm^2)	450		
Area of steel, (mm^2)	741		

* $E_c=4700\sqrt{f'_c}$ ** $f_t=0.62\sqrt{f'_c}$ †Assumed value

Beam B3- Results of Analysis

The experimental and numerical load deflection curves obtained for this beam are exhibited in **Fig. (13)**. This figure shows good agreement for the finite element solutions compared with the experimental results throughout the elastic range of behavior. The figure reveals that the obtained final deflection is slightly greater than the corresponding experimental deflection. The predicted behavior of the load-deflection curve is almost similar to the experimental results. The ultimate load obtained by the finite element method is less than the experimental value by 2.5%, while the ultimate load obtained by direct strain compatibility method is greater than the experimental value by 2.0%, as listed in **Table (4)**.

At total load of 185kN, **Fig. (14)** shows the distribution of the longitudinal stresses along the span length measured at different distance from bottom face of the cross section. From this figure, the critical section is at about 4000mm measured from the support, which represents 26% of the total span.

Table (4) Beam B3 - Predicted cracking and ultimate loads.

Beam B3	*Cracking load (kN)*	*Ultimate load (kN)*
Experimental	*116*	*245*
F.E.M	*110*	*239*

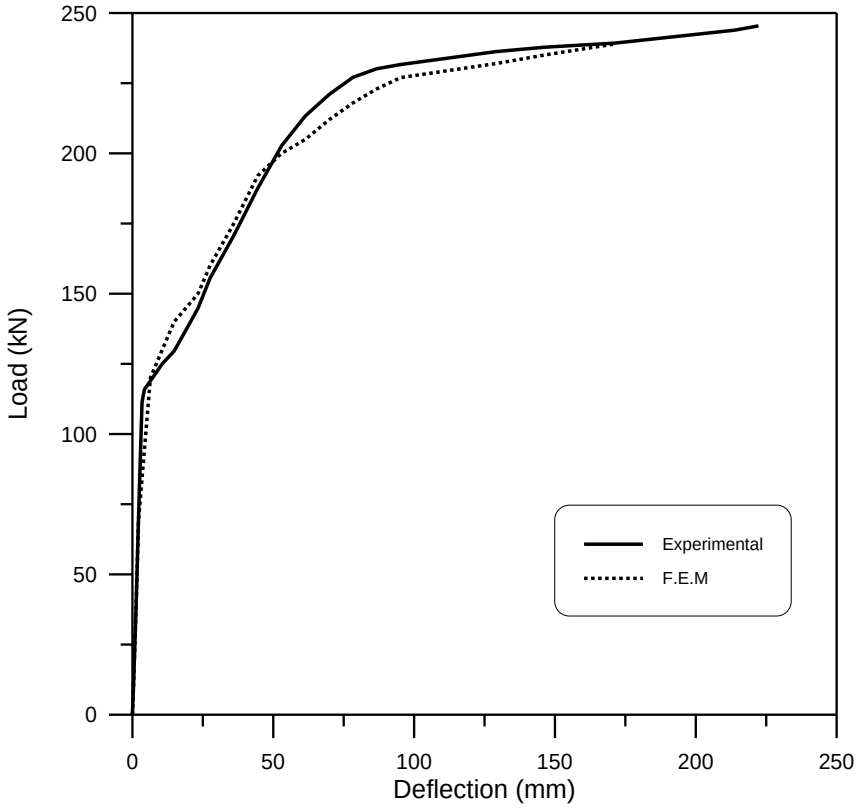

Fig. (13). Beam B3- numerical and experimental total load- midspan deflection behavior.

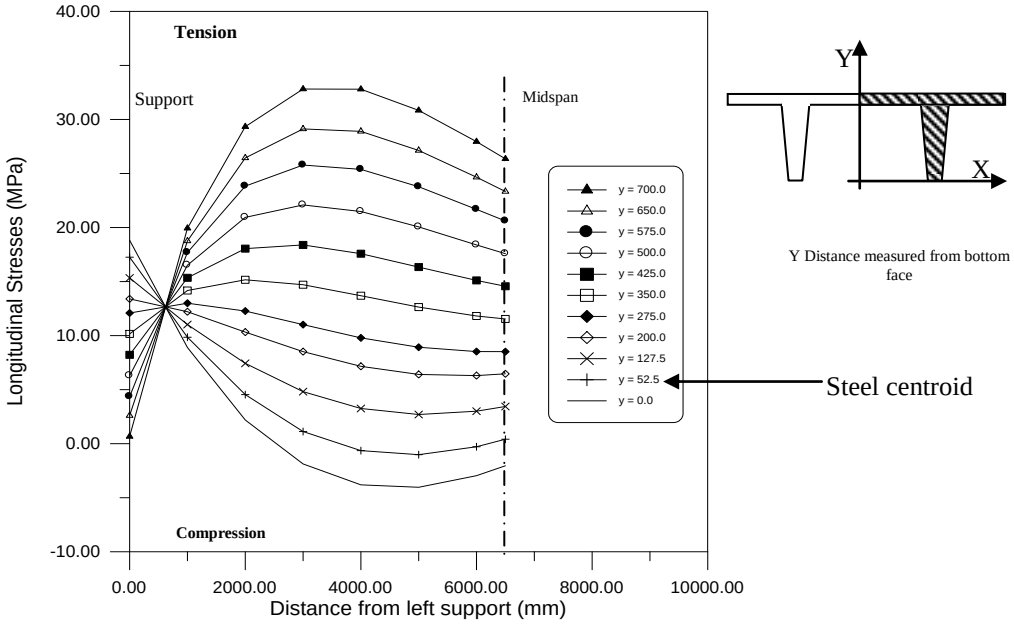

Fig. (14) Beam B3 - variation of longitudinal stresses at different depths along the span length at total load of 185kN.

Parametric Study

To investigate the effect of some material and solution parameters on the nonlinear finite element analysis of prestressed concrete double tee beams in flexure, beam B2 has been chosen to carry out this study. The parameters considered were the mesh refinement, tension-stiffening parameters, concrete compressive strength, amount of prestressing steel reinforcement and initial prestressing forces. In each numerical test, one parameter has been considered to vary while the other parameters being held constants in order to isolate the effects of the parameters considered. In the following sections, the effect of each parameters considered in this study is described.

Effect of Tension-Stiffening Parameters

The variation of tension-stiffening parameters α_1 and α_2 can affect the post-cracking behavior at early stages after cracking of the prestressed concrete members. Numerical analyses for beam B2 with values of α_1, which represents the rate of release of tensile stress as the crack widens, equals to 4, 6, 8, 10, and 12 have been considered. In these tests, α_2 was set equal to 1.0. **Figure (15)** shows that the parameter α_1 has a negligible effect on the collapse load and slightly affects the post cracking flexure stiffness at early stages after cracking. The figure reveals that the best fit to the experimental results was obtained for α_1 equals to 10.0.

To study the effect of the parameter α_2, which represents the sudden loss in the tensile stresses at instant of cracking; numerical analyzed for beam B2 have been carried out with α_2 equals to 0.2, 0.4, 0.6, 0.8, and 1.0. In these tests α_1 was set equal to 10.0.

Results of the analyses also revealed that the parameter of α_2 affects on the behavior at loading stage close to the ultimate load as shown in **Fig. (16)**.

Good agreement with the experimental load deflection curve has been achieved for α_2 equal to 1.0. For α_2 set to be equal to 0.2, 0.4, and 0.6, the response of the numerical load deflection curve was softer than the experimental results.

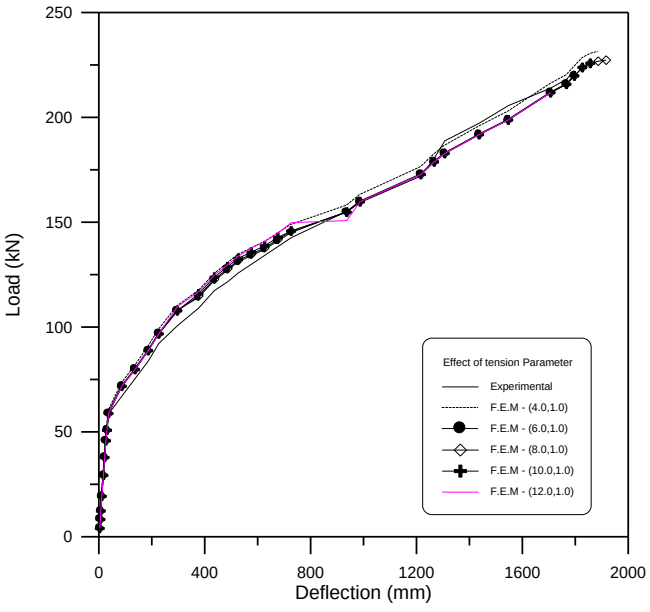

Fig. (15). Beam B2- effect of tension-stiffening parameter (α_1) on the load-deflection response.

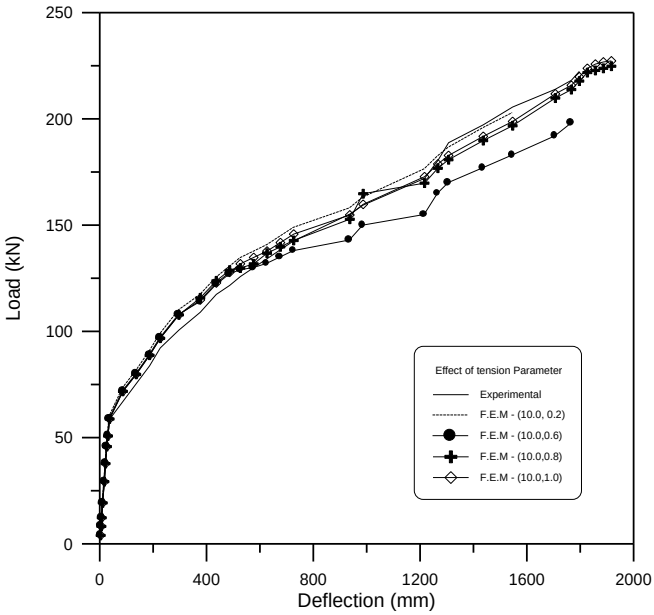

Fig. (16). Beam B2- effect of tension-stiffening parameter (α_2) on the load-deflection response

Effect of Mesh Refinement

Four different finite element meshes have been considered in this study to investigate the effect of the element aspect ratio as shown in **Fig. (17)**. The finite element solutions obtained for the prestressed concrete beam B2 using the different finite element meshes are compared in **Fig. (18)** with the experimental load-deflection curve.

The figure reveals that the numerical load-deflection curves obtained for all meshes considered are almost similar. From these results and as a conclusion, the element aspect ratio does not seem to significantly affect the finite element solutions of prestressed concrete double tee beams under flexure. Therefore, the remaining tests can be carried out using the 10-elements mesh shown in **Fig. (17)**.

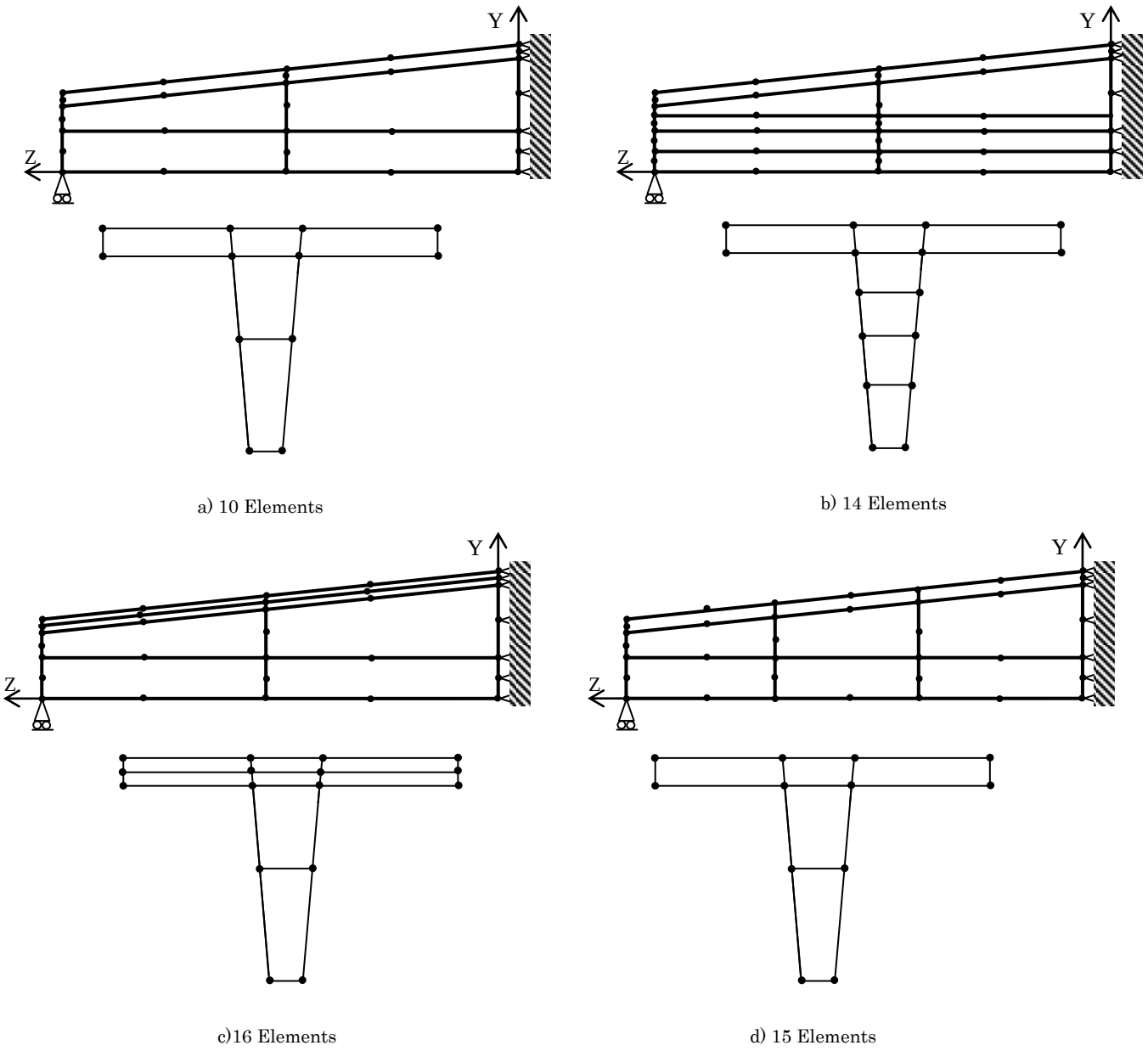

Fig. (17). Types of meshes used in the analysis.

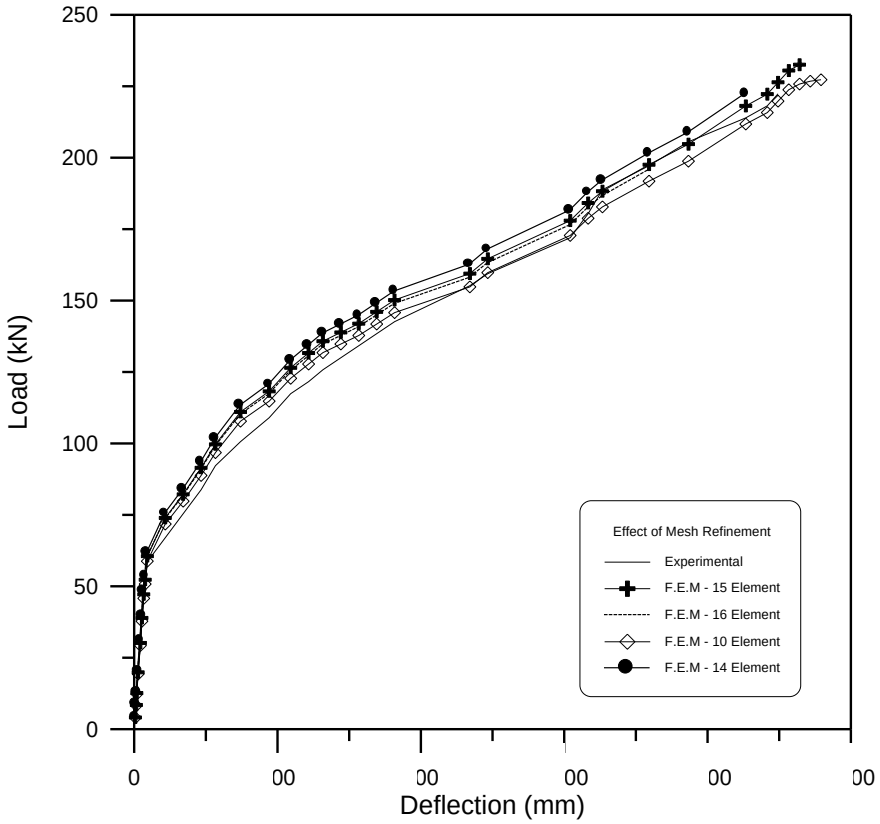

Fig. (18). Beam B2- Effect of mesh refinement on the load-deflection response

Effect of Grade of Concrete.

In order to study the effect of using different values of compressive strength of concrete f_c' on the overall behavior of the prestressed concrete double tee beams, the prestressed concrete beam B2 has been analyzed for different values of f_c'. The values considered were 25, 30, 40, 50, 60, 70, and 90MPa. **Figures (19)** and **(20)** show the effect of this parameter on the response of flanged reinforced concrete beams represented by the load deflection curves.

It is obvious from these two figures that the ultimate capacity of the member increases with the increase of the compressive strength fc'. **Figure (20)** shows the effect of using high strength concrete on the load deflection behavior of the prestressed concrete beam analyzed. Stiffer response has been obtained for higher concrete compressive strength relative to the normal concrete strength. The ultimate capacity of the flanged beams increases slightly with the increase of fc' from 30 to 90 MPa, as shown in **Figs. (19)** and **(20)**. The overall response of the beam is not affected sensibly by the above-mentioned slight increase in the ultimate capacity, whereas failure occurs by yielding of reinforcement before crushing of concrete commences.

Table (5). shows the cracking and ultimate loads obtained for different values of concrete compressive strength, on which the effect of increasing the concrete compressive strength led to higher cracking and ultimate loads. It is found that by increasing the concrete compressive strength from 25 to 50MPa, the cracking load is increased by 16% and the ultimate load is increased by 18%. While when the compressive strength of concrete is increased to 90MPa, the creaking load is increased by 61% and the ultimate load is increased by 25%.

Table (5) Beam B2, cracking and ultimate loads for different values of concrete compressive strength.

Concrete Compressive Strength	*Exp.*	*Analytical*						
	f_c'=45	f_c'=25	f_c'=30	f_c'=45	f_c'=50	f_c'=60	f_c'=70	f_c'=90
Cracking load (kN)	68	62	68	72	72	75	92	100
Ultimate load (kN)	222	198	210	227.5	235	240	245	248

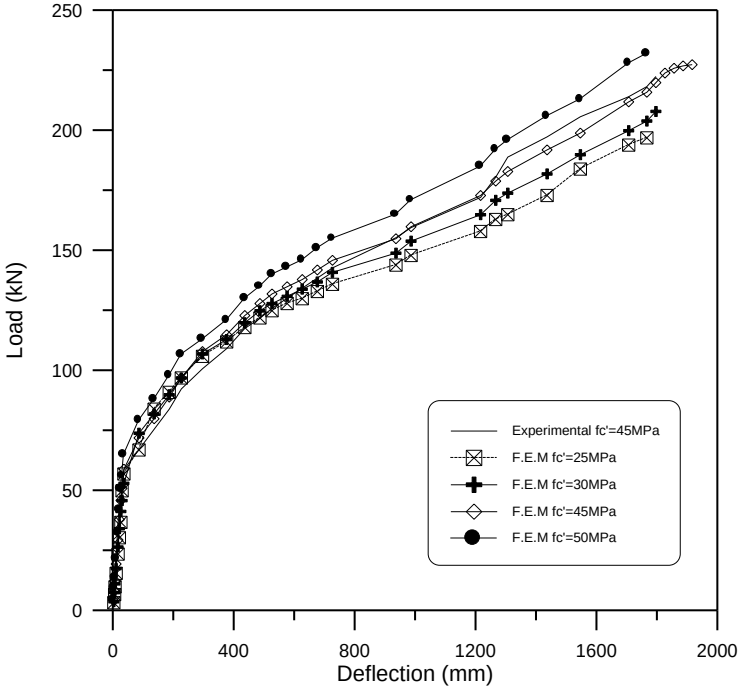

Fig. (19). Beam B2- Effect of concrete compressive strength on the load-deflection response (f_c' from 25-50MPa).

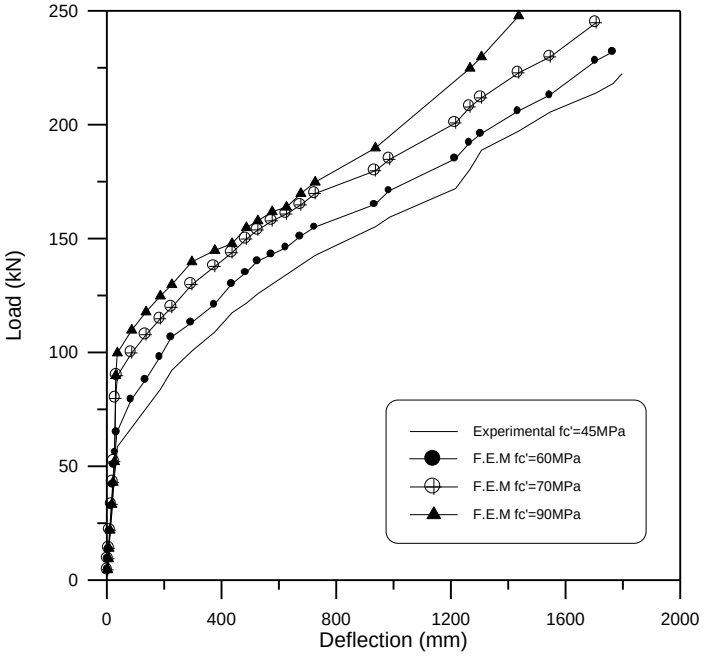

Fig. (20). Beam B2- Effect of Concrete Compressive Strength on the load-deflection response (f_c' from 60-90MPa).

Table (6) shows the ultimate moment capacities obtained for different values of concrete compressive strength predicted by the finite element method compared with the ACI-code values. Obviously shown from this table that as the concrete compressive strength is increased the ACI-code values become more conservative compared with the numerical results. For higher concrete strength '90MPa', the ratio of the predicted ultimate moment to the corresponding ACI-Code values is 1.10.

Table (6) Beam B2-theoretical and numerical ultimate moment

f_c' (MPa)	M_{ACI} (kN.m)	$M_{(F.E.M)}$ (kN.m)	$M_{(F.E.M)} / M_{ACI}$
25	943.00	950.50	1.01
30	943.25	952.68	1.01
45	943.50	971.80	1.03
50	944.00	972.25	1.03
60	944.25	1019.75	1.08
70	944.50	1024.75	1.08
90	945.00	1039.50	1.10

Influence of Effective Prestressing Stress (fse)

In order to study the influence of effective prestressing stress f_{se} on the behavior and ultimate load capacity of prestressed concrete beam B2, different values of the (f_{se}) have been considered. The selected values for this parameter were 800, 950, 1100 and 1200MPa. In this analysis the area of prestressing steel was kept constant. **Figure (21)** shows the analytical load-deflection curves obtained for the selected values of (f_{se}) together with the experimental curve, f_{se}=1117MPa. The results presented in **Fig. (21)** reveal that a stiffer response has been achieved with increasing the value of (f_{se}). The cracking and ultimate loads obtained from this study are listed in **Table (7)**. The table shows that the increase of the effective prestressing stress from 900-1300MPa), led to an increase in the cracking load by 22% and increase in the ultimate loads by about 34%.

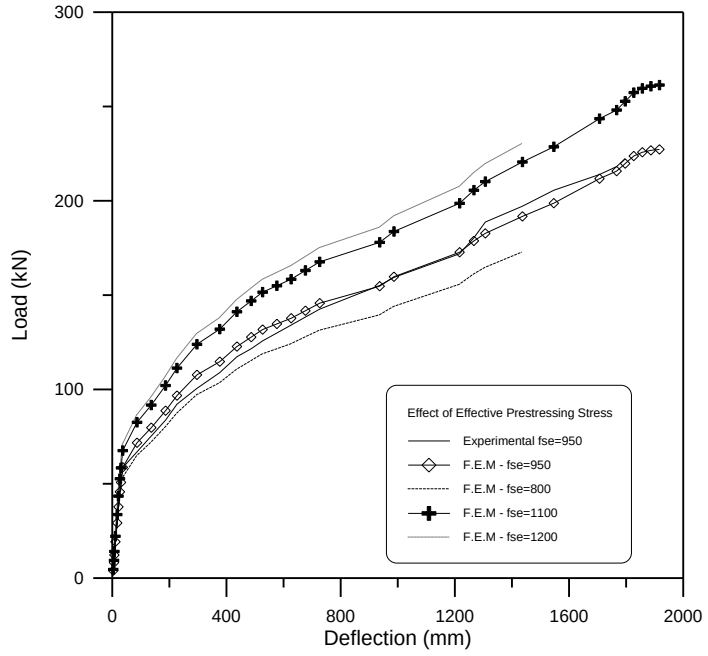

Fig. (21). Beam B2- influence of effective prestressing stress on the load-deflection response.

Table (7) Beam B2, cracking and ultimate loads for different values of effective prestressing stress.

Effective Prestressing stress(MPa)	*Exp.*	*Analytical*			
	f_{se}=1117	f_{se}=900	f_{se}=1117	f_{se}=1200	f_{se}=1300
Cracking load (kN)	68	67	70	72	82
Ultimate load (kN)	222	172	227.5	261.5	232

Effect of Amount of Prestressing Steel (Aps)

Figure (22) shows the effect of amount of prestressing steel on the load-deflection behavior of beam B2. The actual amount of prestressing steel used in the experimental test of this beam was 1718 mm^2. Different values of prestressing steel area have been used in the finite element analysis to approach this aim. These values were 1200, 1500, 1900, and 2100 mm^2. The ultimate flexural capacity of the chosen flanged prestressed beam shows an increase in its value with the increase of the amount of prestressing steel. The finite element solutions reveal that the cracking load and the post cracking stiffness of the tested beam are substantially increased. The cracking and ultimate loads obtained from this study are listed in **Table (8)**. Obviously shown from this table that the increase of the amount of prestressing steel by 75% (i.e from 1200-2100MPa), led to an increase in the cracking loads by 30% and an increase in the ultimate load by 40%.

Table (8) Beam B2, cracking and ultimate loads for different amount of prestressing steel.

Amount of prestressing steel mm^2	*Exp.*	*Analytical*				
	1718	*1200*	*1500*	*1718*	*1900*	*2100*
Cracking load (kN)	68	57	65	70	72	75
Ultimate load (kN)	222	180	208	227.5	242	258

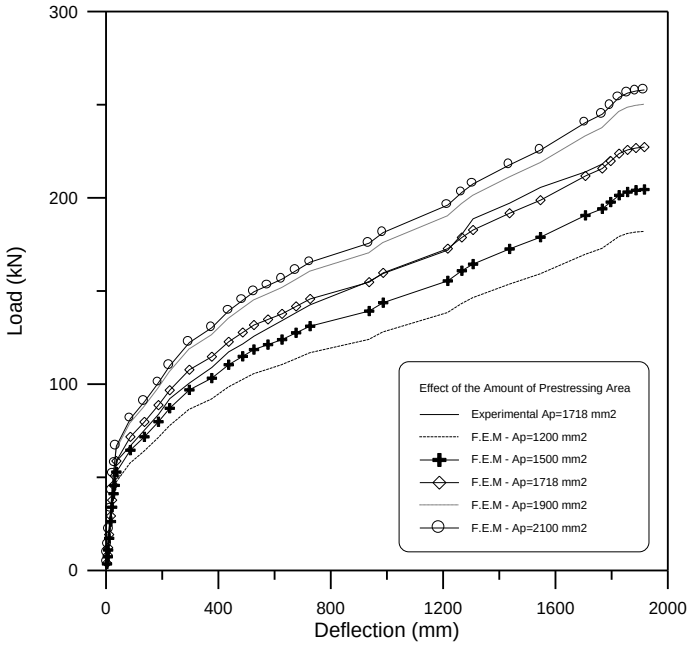

Fig. (22). Beam B2- effect of amount of prestressing area on the load-deflection response.

Conclusions

1- The three-dimensional nonlinear finite element model adopted in the present work is suitable to predict the behavior of prestressed concrete double tee beams under flexure. The model which has been proposed in the present research work to simulate the prestressing effects by introducing initial effective prestressing stresses and strains to the sampling points that represent the prestressing tendons is suitable for analyzing such beams. The numerical results showed that the predicted load-deflection behavior and the collapse loads are in good agreement with the experimental results.

2- According to the finite element analyses carried out in the present study, it is notable that the ultimate load is increased substantially by about 34% when the values of the effective prestressing stress (fse) increased from 900MPa to 1300MPa with a constant area of prestressing steel (Aps).

3- In general, the magnitude of the concrete compressive strength affects the overall load-deflection behavior of non-prismatic prestressed concrete beams. As the concrete compressive strength increases from 25MPa to 90MPa, the ultimate load capacity increases by about 25%.

4- For the analyzed non-prismatic double tee beams, the finite element results show that when the area of prestressing reinforcement increases from 1200 mm2 to 2100 mm2, the ultimate load capacity increases by about 40%.

5- For high strength concrete, the predicted ultimate moment of the analyzed double tee beams, is about 10% higher than the ultimate moment obtained using the ACI 318M-02 Code formulae. The ACI Code values have been found to be conservative for high values of concrete compressive strength.

References

1. Structural Precast/Prestressed Concrete "Technical Brochure" Canadian Precast/Prestressed Concrete Institute", Internet Reference.www.cpci.com.
2. Wright H.E., and Burns N.H., "Deflection of double tees and hollow-cored slabs with high tension allowed in concrete", PCI journal, July-August ,1974
3. Burnley G.and Aswad A., "Omission of web reinforcement in Prestressed double tees", PCI journal,March-April,1989.
4. El Shahawy, M.," Feasibility Study of Transversely Prestressed Double Tee Bridges," PCI Journal,V.6,No.1,Sep.-Oct.1990,pp.56-69.
5. Al-Fayhaa Company for Precast Unit, Experimental Report Presented by The Engineering consultant office on AL-Basra University, Nov.1992.
6. Tadros M.,Einea A.,"Design and Performance Testing of Prestressed Precast Reinforced Concrete Double Tee Beams with Web Openings," Center of Infrastructure Research, on Internet, http://www.cir.unomaha.edu/index.htm –1999
7. Nass W.T.,Jr.," Design of Prestressed Precast Double Tee Sections", M.S Thesis, University of Florida, Summer 1999. 37.ACI-Committee 318,"Building Code Requirements for Structural Concrete (ACI 318M-95)and Commentary (ACI 318RM-95)", American Concrete Institute,Detroit,Michigan,1995.
8. Karbala Company for Precast Concrete Unit, Experimental Report Presented by The National Center for the construction Laboratories,Sep.2002.
9. Grace N.F.et al., "Experimental Study and Analysis of a Full-Scale CFRP/CFCC Double Tee Bridge Beam, "PCI Journal,V.5,No.2, July-Aug.2003,pp.120-139.
10. Paolo Casadei, Antonio Nanni, "SRP Strengthening of PC Double Tee Beams" Research Supply to University Repair of Building & Bridges with Composites Center (RB2C)–June 2004.
11. Al-Shaarbaf, I. A. S., “Three-dimensional nonlinear finite element analysis of reinforced concrete beams in Torsion”, Ph.D. Thesis, University Of Bradford, 1990.
12. Mohammed, Hussam A., "Experimental and Nonlinear Analysis of Non-Prismatic Double Tee Prestressed Concrete Beams" PhD Thesis, Baghdad University, Sep. 2005.

Notations

α_1, α_2	Tension stiffening parameters
β	Shear retention factor or material constant
γ	Shear strain
$\gamma_1, \gamma_2, \gamma_3$	Shear retention parameters
ε	Strain
ε_{cu}	Concrete ultimate strain
ε_e	Elastic strain
ε_o	Strain corresponding to peak uniaxial concrete compressive stress
ε_p	Plastic strain
λ	Reduction factor
ν	Poisson's ratio
σ	Stress